### **FLUORIDE**

Quarterly Journal of The International Society for Fluoride Research Inc.

# Regional Economic Collaborative Governance as a Medium for Fluoride Pollution Prevention and Control: Study based on Balanced Path between Industrial Layout and Economic Development under the Guidance of Public Health

Unique digital address (Digital object identifier [DOI] equivalent): https://www.fluorideresearch.online/epub/files/404.pdf

Bian TANG<sup>1</sup>, Qiao PENG<sup>2\*</sup>, Yuelan SHI<sup>3</sup>, Utpal Singh VERMA<sup>4\*\*</sup>

- School of Management, Guilin University of Aerospace Technology, Guilin 541004, Guangxi, China
- <sup>2</sup> School of Statistics, Tianjin University of Finance and Economics, Tianjin 300221, China
- <sup>3</sup> School of Political Science and Public Administration, Guangxi Normal University, Guilin 541004, Guangxi, China
- <sup>4</sup> Department of Agriculture, G.B. Pant Degree College, Kachhla, Badaun 243636 (U.P.), India

### Corresponding author:

\* School of Statistics, Tianjin University of Finance and Economics, Tianjin 300221, China

Email: penggiao25@outlook.com

\*\* Department of Agriculture, G.B. Pant Degree College, Kachhla, Badaun 243636 (U.P.), India

Email: utpal.verma11@gmail.com

Submitted: 2025 Aug 03 Accepted: 2025 Sept 30 Published as e404: 2025 Oct 08

### **ABSTRACT**

**Purpose:** This study addresses the spatial mismatch between regional fluoride pollution emission intensity and health risks and proposes an optimized industrial layout approach mediated by multi-agent collaborative governance.

**Methods:** Using 11 provinces and municipalities within the Yangtze River Economic Belt as empirical research areas, a comprehensive analytical framework is constructed, integrating spatial econometric modeling (spatial Durbin model), multi-objective optimization (NSGA-II algorithm), and dynamic system simulation.

**Results:** The framework quantifies the spatial spillover effects of industrial specialization (locational entropy) and economic density on fluoride emissions and optimizes industrial migration pathways to balance public health and economic development goals. Under the collaborative governance scenario, the frequency of regional fluoride emissions exceeding the standard decreases from 18.2% in 2015 to 4.3% in 2022, and the DALYs lost decrease from 1,35,200 person-years to 86,700 person-years.

**Conclusions:** The collaborative economic governance can effectively address the spatial mismatch between high pollution and low health outcomes.

**Keywords:** Industrial layout; Economic development; Fluoride contamination; Management; Regional economic governance

### INTRODUCTION

As the global economic landscape undergoes profound changes, the relationship between regional economic integration and local government governance is becoming a key factor in promoting sustainable regional economic development.<sup>1</sup> The indepth study on the regional cooperative governance of Pangkalpinang city analyzing its role and strategic significance in urban economic development.<sup>2</sup> Gianelle et al.<sup>3</sup> demonstrated the current situation, existing challenges and economic impact of regional innovation policy governance, and proposed that good regional innovation policy governance can promote

regional economic growth and enhance regional competitiveness. The COVID-19 epidemic has had a huge impact on the global economy, and the resilience of the regional economy has become a focus of attention. China, as an example to analyze the relationship between governance capacity, related diversity and regional economic resilience. While fiscal decentralization and good governance positively impact Indonesia's regional economic growth, further optimization of the decentralization mechanism and enhancements to the quality of governance are needed. 5

The impact of entrepreneurship and governance quality on global and regional economic performance has attracted attention in the context of globalization and sustainable development. The entrepreneurship and high-quality governance have a significant role in promoting global and regional economic performance and an important way to achieve sustainable development. The role and function of large regional trade agreements in global economic governance.<sup>6,7</sup> Ekeocha et al.8 analyzed the relationship between economic policy uncertainty, governance institutions and economic performance and their regional differences. The impact of local governance and regional self-owned income on economic growth and found that good local governance and stable selfowned income sources can promote economic growth.9 Suhendra10 demonstrated the in-depth study on SIPDD innovation and ARABIKA cabinet projects, analyzing their innovations and effects in regional development governance.

Fluoride (F) contamination, a typical industrially derived emerging pollutant, often exhibits a significant mismatch between its emission intensity and the resulting health risks. High-emission regions do not necessarily have high health risks, whereas low-emission regions can bear a greater disease burden due to dense populations or fragile environments. This mismatch stems from the disconnect between industrial layout, environmental regulation, and public health objectives in traditional governance models.

This article considers regional economic collaborative governance as a vehicle for F pollution prevention and control. It constructs an industry-pollution-health chain analysis model to reveal the transmission mechanism by which economic density and industrial specialization influence health risks through spatial spillover effects. By coupling a spatial econometric model (the spatial Durbin model), multi-objective optimization (the NSGA-II algorithm), and dynamic system simulation, it quantifies the trade-offs of industrial migration, achieving a closed-loop analysis from diagnosis to regulation.

The present paper explores the mechanism and practical path of regional economic collaborative governance in the prevention and control of F pollution, and reveals how to achieve scientific adjustment of industrial layout and sustainable economic development through collaborative governance under the guidance of public health.

### **METHODOLOGY**

### **Research Area and Data**

This study selected 11 provinces and municipalities within the Yangtze River Economic Belt as the empirical region. This region, spanning the eastern,

western regions, exhibits typical central, and characteristics of gradient development. Its comprehensive industrial chain provides an ideal sample for studying the relationship between industrial layout and pollution. To ensure the comprehensiveness and accuracy of the data, this study constructed a multi-source, multi-dimensional comprehensive data system. Industrial economic data are primarily sourced from the 2015-2022 provincial and municipal statistical yearbooks and the National Bureau of Statistics' industrial enterprise database. By aggregating enterprise micro-data at the prefecturelevel, it calculates each city's industrial added value, location entropy for high-fluorine-emitting industries, such as the fluorine chemical industry, ceramics, and aluminum electrolysis, and economic density. 11,12

The location entropy calculation formula, as stated:

$$LQ_{ij} = \frac{(E_{ij}/E_j)}{(E_i/E)}$$
 (1)

 $E_{ij}$  is the industrial added value of industry i in prefecture-level city j,  $E_j$  is the total industrial added value of prefecture-level city j,  $E_i$  is the industrial added value of industry i in the entire study area, and E is the total industrial added value of the entire study area.

The construction of the F emission inventory integrates the key pollution source data in the annual environmental statistics report and the information from the national pollution source census, and crosschecks and verifies the two. The population spatial distribution data uses 1×1 km grid data corrected in combination with land use types to reflect the actual exposure of the population. The prevalence data of endemic fluorosis, such as dental and skeletal fluorosis are systematically collected from the annual work reports of the provincial and municipal centers for disease control and prevention.

Meteorological data, such as wind speed, wind direction, ambient air temperature, and mixing layer height are from the National Meteorological Information Center (NMIC), and the terrain data uses a digital elevation model with a resolution of 30 meters. All data are uniformly spatially aligned, interpolated, and outlier detected and cleaned through the ArcGIS and Python platforms, ultimately forming a set of prefecture-level city panel data sets that are continuous in time and space and have unified standards. During the data integration process, in order to ensure the spatial consistency of data from different sources, coordinate system integration and resampling are performed. The resampling process is as follows:

$$V_{target} = \frac{\sum_{i=1}^{n} w_i \cdot V_{source_i}}{\sum_{i=1}^{n} w_i}$$
 (2)

Table 1. Emission characteristic parameters of high fluorine emission industries

Industry type	Average emission factor (kg/ton product)	Typical emission height (m)	Emission temperature (K)
Fluorochemical industry	0.18	35	420
Ceramic manufacturing	0.10	25	380
Aluminum electrolysis	0.15	40	450
Thermal power generation	0.06	100	480
Glass manufacturing	0.08	20	390

 $V_{target}$  is the value of the target grid cell,  $V_{source_i}$  is the value of the i-th source grid cell, and  $w_i$  is the weight determined by the sampling method.

### **Construction of Core Analysis Framework**

This study constructs a comprehensive analytical framework integrating the industry-pollution-health chain to quantify the ultimate impact path of industrial economic activities on public health. 13,14 First, in terms of quantifying industrial linkages, based on inter-regional input-output tables and enterprise-level supply chain data, a complex network analysis method is applied to calculate the linkage coefficients of specific industries between cities. A directed weighted network with prefecture-level cities as nodes and industrial linkages as edges are constructed to depict the spatial topological structure of regional industrial collaboration. The strength of the linkage between nodes can be quantified by the linkage coefficient:

$$R_{ij}^{k} = \frac{F_{ij}^{k}}{\sqrt{F_{i}^{k} \cdot F_{j}^{k}}}$$
 (3)

 $F_{ij}^k$  represent the total factor flow of the industry between the two cities, while  $F_i^k$  and  $F_j^k$  represents the total outflow of the industry in city i and city j, respectively.

The CALPUFF model is used to simulate pollutant dispersion. This model effectively handles pollutant transport and transformation in complex terrain, such as hills and river valleys, and in local circulation conditions, such as sea-land breezes and valley-valley winds. Simulation inputs include a high-resolution spatial and temporal emission source inventory (point and area sources), hourly meteorological fields (generated by the WRF model), and high-precision digital elevation model. CALPUFF simulates the spatiotemporal dynamic distribution of F ground concentrations by coupling the Gaussian plume dispersion algorithm with a terrain dynamics module. Its core diffusion formula is as:

$$C(x,y,z) = \frac{Q}{2\pi u \sigma_y \sigma_z} exp\left(-\frac{y^2}{2\sigma_y^2}\right) \left[exp\left(-\frac{\left(z-H_e\right)^2}{2\sigma_z^2}\right) + exp\left(-\frac{\left(z+H_e\right)^2}{2\sigma_z^2}\right)\right] \tag{4}$$

C(x,y,z) is the pollutant concentration at the receptor point (x,y,z), Q is the pollution source intensity, u is the wind speed,  $\sigma_y$  and  $\sigma_z$  are the horizontal and vertical diffusion parameters, respectively, and H is the effective emission height of the smoke plume.

Table 1 shows the emission characteristic parameters of high-fluorine-emitting industries. Finally, in the health loss assessment phase, the World Health Organization-recommended disability-adjusted life years (DALYs) are introduced as a quantitative indicator. By reviewing epidemiological literature, a dose-response function is established between F exposure concentration and the incidence of skeletal and dental fluorosis.

Fluoride concentration raster data output by CALPUFF simulations are spatially overlaid with population distribution raster data. Healthy life years lost due to F exposure are calculated on a grid-by-grid basis and summarized to obtain regional total DALYs. 15,16

### **Spatial Econometric Analysis**

To analyze the interaction and spillover mechanism between industrial layout and F pollution in the spatial dimension, the Spatial Durbin Model (SDM) is used for empirical testing. The model setting uses the F emission intensity of each prefecture-level city as the core dependent variable, and the core independent variables include the location entropy index representing the degree of industrial specialization and the economic density representing the intensity of economic activities.

At the same time, the model introduces control variables, such as the technological progress index reflecting the level of clean production (proxied by the number of patents) and the intensity of environmental regulation representing policy pressure (measured by the proportion of environmental protection investment in GDP). <sup>17,18</sup> Table 2 shows the descriptive statistical results of the core variables of the Spatial Durbin Model.

Table 2. Descriptive statistics of core variables in the spatial Doberman model

Variables	Units	Mean	Std. Dev.	Min	Max
Fluoride emission intensity (Y)	Regional F emissions/ area (t/km²)	0.85	0.62	0.12	3.41
Location quotient (LQ)	Specialization in high-F industries (dimensionless)	1.02	0.48	0.31	2.87
Economic density (ED)	Industrial added value per unit area (10,000 yuan/km²)	2480.5	18230.5	312.8	8950.2
Tech progress (InPatent)	Annual patent grants (natural log)	5.54	1.23	2.30	8.91
Environmental regulation (ERI)	Environmental investment as GDP (%)	1.21	0.45	0.38	2.85

Spatial Doberman model formula is as:

$$Y = \rho WY + X\beta + WX\theta + \epsilon \tag{5}$$

Y represents the dependent variable vector (F emission intensity), X represents the matrix of independent variables (including location entropy, economic density, and control variables), W represents the spatial weight matrix, p represents the spatial autoregressive coefficients.  $\beta$  and  $\theta$  represents the coefficient vectors of the independent variables and their spatial lags, respectively.  $\epsilon$  represents the random error term.

A composite weight matrix combining geographic contiguity and economic interconnectedness is used to capture spatial dependence and spillover effects across administrative boundaries. To mitigate the potential endogeneity between industrial structure and pollution emissions, it selects exogenous policy dummy variables, such as each city's historical industrial base and whether it is designated a national circular economy or eco-industrial demonstration park, as instrumental variables. A two-stage least squares method is used for parameter estimation. The model's estimated results are further decomposed using partial differentiation into direct effects (the impact of a city's industrial economic activities on its pollution) and indirect effects (the impact of economic activities in neighboring or economically connected cities on its pollution), thereby revealing the necessity and potential paths for regional collaborative governance.

### **Multi-objective Optimization Model Design**

Based on the patterns revealed by spatial econometric analysis, it further designs a multi-objective optimization model for regional industrial layout that is public health-oriented and considers multi-agent collaboration. The objective function of this model contains two conflicting objectives that need to be optimized simultaneously, i.e., one is the public health objective, namely minimizing the overall

regional F exposure health risk  $f_1$ , specifically defined as the proportion of the population whose drinking water F concentration exceeds the WHO recommended limit (1.5 mg/L).

$$minf_1 = \frac{\sum_{r=1}^{R} P_r \cdot I(C_r > 1.5)}{\sum_{r=1}^{R} P_r}$$
 (6)

 $P_{\rm r}$  is the population of the r-th subregion, and  $C_{\rm r}$  is the average F concentration in the drinking water of the r-th subregion.

The second is the economic development goal, which is to maximize the average annual growth rate  $f_2$  of regional industrial added value during the study period, as follows:

$$\max f_2 = \left(\frac{IVA_T}{IVA_0}\right)^{\frac{1}{T}} - 1 \tag{7}$$

 $IVA_0$  refers to the regional industrial added value during the base period,  $IVA_T$  refers to the regional industrial added value during period T, and T refers to the total number of periods included in the study period

The model's decision variables are set as the proportion and direction of capacity transfer or acquisition of high-F-emitting industries in each city. The optimization process must meet multiple constraints, such as the primary one is the hard constraint of health risk, meaning that the optimized layout must ensure that F exposure levels for the population in each sub-district remain below the acceptable risk threshold:

$$\frac{1}{P_{m}} \sum_{s=1}^{S} P_{ms} \cdot C_{ms} \le R_{m}^{acc} \ \forall m$$
 (8)

 $P_{m}$  refers to the total population of the m-th risk zone,  $P_{ms}$  refers to the population of the s-th subregion within the m-th risk zone,  $C_{ms}$  refers to the average F concentration in drinking water in the s-th sub-region within the m-th risk zone, and  $R_{mc}^{acc}$  refers to

the acceptable F exposure risk threshold set for the m-th risk zone.

Secondly, there is the economic feasibility constraint, which ensures that fluctuations in the regional industrial chain completeness index (ECI, calculated based on the input-output table) remain within a reasonable range to avoid industrial chain disruptions due to industrial relocation. The constraints are as:

$$\left| \frac{\mathsf{ECI}_{\mathsf{t}} - \mathsf{ECI}_{\mathsf{0}}}{\mathsf{ECI}_{\mathsf{0}}} \right| \le \delta \tag{9}$$

ECI $_0$  refers to the regional industrial chain completeness index in the base period, ECI $_t$  refers to the regional industrial chain completeness index in period t, and  $\delta$  refers to the maximum relative volatility allowed by the industrial chain completeness index.

Furthermore, socioeconomic constraints, such as guaranteed growth rate for industrial added value must be set. The model is solved using the NSGA-II (non-dominated sorting genetic algorithm). By simulating the selection, crossover, and mutation processes of biological evolution, it conducts a global search under complex constraints, ultimately generating a Pareto-optimal solution set that depicts the trade-off between economic growth and health risks under varying intensities of industrial migration.

### **RESULTS AND DISCUSSION**

### **Descriptive Statistics and Spatial Pattern Analysis**

Spatial interpolation of point and area source emission data is performed using the inverse distance weighted (IDW) method, with parameters set to a power exponent of 2, a neighborhood search radius of 50 km, and maximum number of neighborhood points of 15. This generates a  $1\times 1$  km resolution raster. The raster data is aggregated to prefecture-level city units using the Zonal Statistics tool, and average values are calculated for each city. Key indicators are extracted

and descriptive statistical tables are constructed to illustrate the spatial pattern characteristics of representative cities (Table 3).

Tabular analysis reveals significant spatial mismatches, i.e., regions with high F emission intensities (Hefei, 1.18 t/km²) are geographically aligned with high health risks (dental fluorosis prevalence of 14.6%), suggesting that industrial agglomeration (locational entropy of 1.78) directly exacerbates local exposure risks. However, high-density economic regions, such as Shanghai (economic density of 152 million yuan/km²), due to technological advancements and strict environmental regulations, have emission intensities of only 0.32 t/km² and the lowest prevalence (4.8%), forming high economy, low pollution pattern.

In contrast, some central and western cities (Wuhan), despite high levels of industrial specialization (locational entropy of 1.48), experience significantly higher health risks (11.8%) than eastern coastal areas due to lagging governance capacity, highlighting the urgency of coordinated regional governance. This mismatch stems from the failure to internalize environmental externalities associated with industrial transfer, necessitating cross-regional policy coordination and optimization.

### **Spatial Doberman Model Regression Results**

A regression analysis is conducted using the Spatial Durbin Model (SDM) on panel data from prefecture-level cities in 11 provinces and municipalities within the Yangtze River Economic Belt. A composite weight matrix (weight ratio 6:4) of geographic proximity and economic connections is used to capture cross-regional spatial dependence. Parameters are estimated using a two-stage least squares method. Historical industrial base and national eco-industrial demonstration park policies are selected as instrumental variables to address endogeneity. The regression results are decomposed into direct effects (the impact of local industrial activities) and indirect effects (spatial spillovers) using partial differentiation.

**Table 3.** The detailed statistics analysis of F pollution, industrial layout and health risks in some prefecture-level cities in the Yangtze River Economic Belt

City	F-emission intensity (t/km²)	Location quotient	Economic density (10 <sup>4</sup> yuan/km²)	Dental fluorosis prevalence (%)
Shanghai	0.32	0.82	15,200.0	4.8
Suzhou	0.75	1.32	9,800.5	7.9
Hangzhou	0.40	0.95	8,600.3	5.1
Hefei	1.18	1.78	3,600.8	14.6
Wuhan	0.92	1.48	4,300.6	11.8

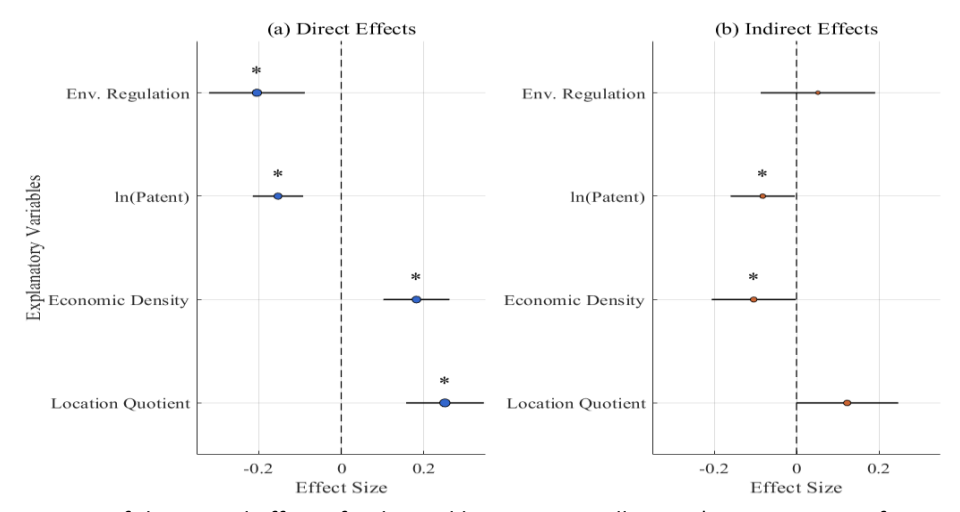


Figure 1. Decomposition of the spatial effect of industrial layout on F pollution. \* represent significant effect

The detailed effect decomposition is shown in Figure 1. Furthermore, the strength of the instrumental variables are tested using a one-stage F statistic (critical value 10). The validation results are shown in Figure 2. Figure 1a shows that the direct effect of locational entropy is significantly positive (0.251, 95% CI: 0.157–0.345), indicating that 1-unit increase in the specialization of high-F-emitting industries leads to 25.1% increase in local F emission intensity, making it the core driving factor.

The direct effect of economic density is 0.182 (95% CI: 0.102–0.262), reflecting that industrial expansion exacerbates local pollution loads. The direct effects of technological progress (InPatent) and environmental regulation (ERI) are -0.153 and -0.204, respectively, indicating that innovation investment and policy constraints effectively suppress local emissions. Figure 1b reveals key spatial spillover mechanisms, the indirect effect of economic density is -0.104 (95% CI: -0.206–0.002), indicating that neighborhood industrial agglomeration generates negative spillovers through technology diffusion.

However, the indirect effect of locational entropy reaches 0.123, suggesting that industrial specialization carries the risk of pollution transfer, such as the relocation of high-F industries to areas with weaker

regulation, leading to cross-border pollution. Industrial specialization is the primary cause of local pollution, while neighborhood economic agglomeration mitigates pollution through knowledge spillovers. It must be vigilant against the negative externalities caused by industrial transfer and establish a cross-domain coordinated regulatory mechanism.

Figure 2 shows that the first-stage F-statistics for all three instrumental variables are significantly above the critical value for weak instrumental variables (F=10). The F-value for historical industrial base is 25.6 (p<0.001), reflecting the strong explanatory power of industrial heritage on current industrial layout, the Fvalue for eco-industrial park policies is 18.3 (p<0.001), confirming that policy intervention effectively drives industrial spatial restructuring and the combined Fvalue reaches 32.7 (p<0.001). The gradient distribution of F-statistics (25.6 $\rightarrow$ 18.3 $\rightarrow$ 32.7) is consistent with theoretical expectations historical path dependence has stronger explanatory power than single policy, but the synergistic effect of policy and historical factors are the strongest. The instrumental variables have passed validity tests, confirming the robustness of the causal inference between industrial layout and pollution emissions.

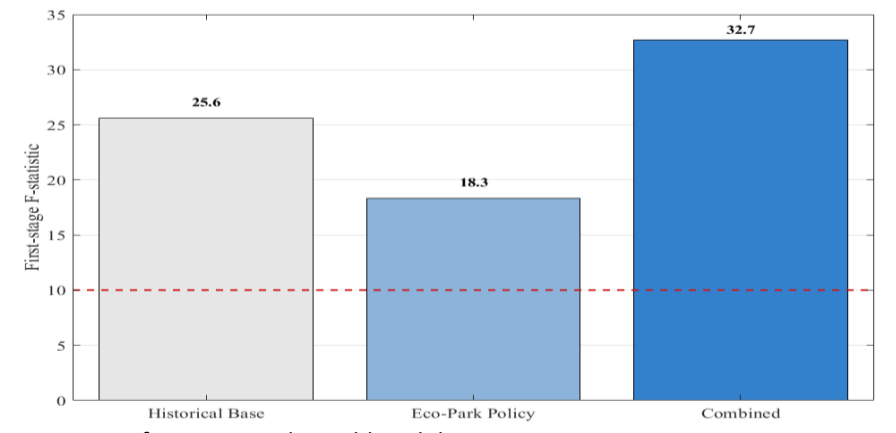


Figure 2. One-stage statistics of instrumental variable validity test

Table 4. Multi-objective optimization results of industrial layout

Scheme	Industry migration intensity (%)	Health risk reduction (%)	Economic growth rate (%)	Industrial chain volatility (%)
S1	10.2	12.3	4.5	1.8
S2	25.6	28.1	6.2	3.5
\$3	30.4	34.7	5.8	4.9
S4	41.3	37.9	5.1	7.2
<b>S</b> 5	50.0	38.7	4.9	8.6

### **Analysis of Multi-Objective Optimization Results**

The NSGA-II algorithm is used to solve the multiobjective optimization model for industrial layout. The parameters are set to population size of 200, a crossover probability of 0.9, and mutation probability of 0.05. The Pareto frontier solution set is generated after 500 iterations. Five typical scenarios are selected, and the reduction in health risks and the change in economic growth rate under each scenario are calculated (Table 4).

As the intensity of industrial relocation increases from 10.2 to 50.0%, the reduction in health risks increases from 12.3 to 38.7%, but the economic growth rate does not increase simultaneously. At the same time, the volatility of the industrial chain increases significantly from 1.8 to 8.6%. This suggests that excessive pursuit of health benefits comes at the expense of robust economic growth and industrial chain security. The S2 option achieves 28.1% reduction in health risks while maintaining high economic growth rate of 6.2% and low industrial chain volatility (3.5%), demonstrating better balance. Therefore, industrial relocation adjustments are not necessarily about greater relocation intensity; the key lies in finding the optimal balance between reduced health

risks and stable economic development. The moderate relocation strategy represented by the S2 option is more feasible path to achieving regional coordinated governance.

## **Empirical Evaluation of Collaborative Governance Paths**

This study constructs a dynamic system simulation model to simulate the F pollution control pathways in the Yangtze River Economic Belt from 2015 to 2022. The Monte Carlo method is used to generate 10,000 parameter perturbations, with the industrial synergy coefficient (0.35-0.85), environmental regulation intensity (1.2-2.8), and public health weight (0.4-0.9) set as key variables. By coupling the CALPUFF atmospheric diffusion model, regional input-output model, and health risk assessment module, the environmental, economic, and health effects of the collaborative governance scheme are quantified. The simulation uses a fourth-order Runge-Kutta method to solve the differential equations, and the comparison is to the baseline scenario, maintaining the existing industrial layout and environmental regulation intensity, with no collaborative governance measures. The output results are shown in Figures 3-5.

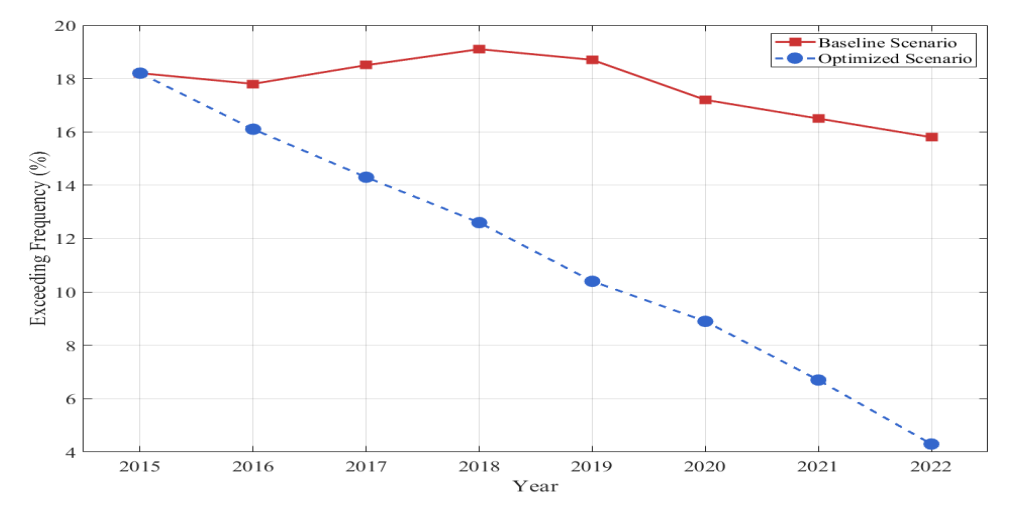


Figure 3. Frequency of F exceeding standards.

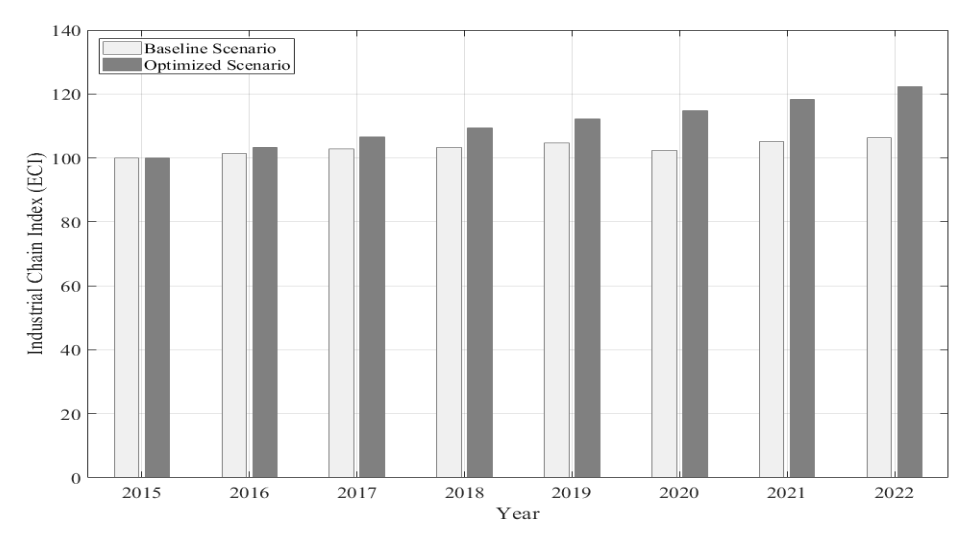


Figure 4. Influence of regional industrial chain completeness index

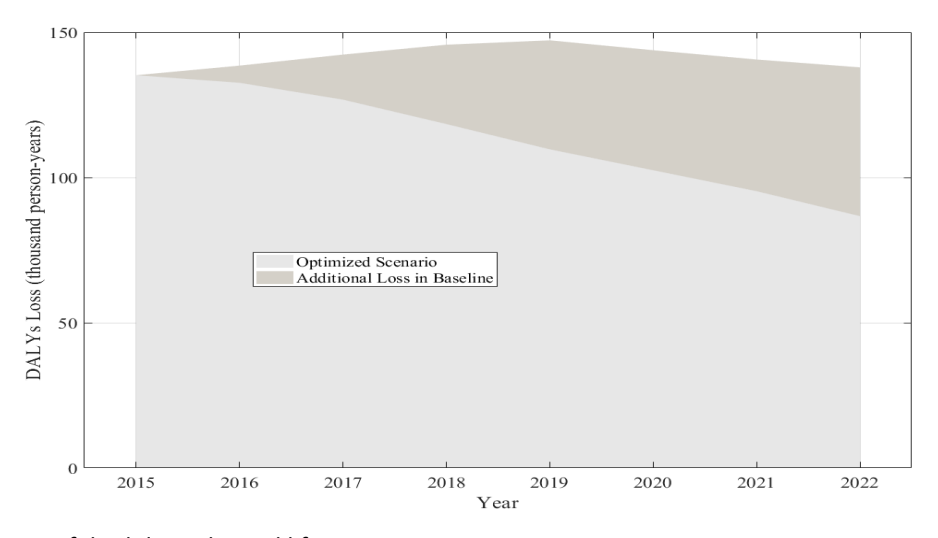


Figure 5. The impact of disability-adjusted life years

The frequency of F violations under the optimized scenario shows a continuous downward trend, falling from 18.2% in 2015 to 4.3% in 2022. While the baseline scenario experiences slight fluctuations in some years (2017-2019), the overall decline is limited (still 15.8% in 2022). This change suggests that the optimization strategy has significant cumulative effect environmental governance, related on to technological upgrades or strengthened control measures. Analysis of the magnitude of the differences shows that the gap between the optimized scenario and the baseline scenario has widened year by year, from an initial zero difference to 11.5% in 2022, highlighting the long-term efficiency-enhancing effect of the optimization measures. Furthermore, the baseline scenario experiences abnormal fluctuations (the frequency first increases and then decreases), possibly due to interference from external factors, while the optimized scenario maintains a steady decline, indicating stronger ability interference.

Economic benefit data shows that the Industrial Chain Index (ECI) under the optimization scenario steadily increases from baseline value of 100.0 in 2015 to 122.4 in 2022, while the baseline scenario experiences more gradual growth (reaching only 106.4 during the same period). The difference between the two scenarios widens from 1.7 in 2016 to 16.0 in 2022. This linear growth trend reflects the sustained and cumulative impact of the optimization strategy on industrial chain integrity. The accelerated growth in the optimization scenario after 2020 is particularly related to the optimization of industrial structure or improved investment efficiency. From volatility perspective, the baseline scenario experiences brief decline in 2020 (ECI dropped from 104.6 to 102.3), influenced by economic cycles or external shocks. The optimization scenario maintains consistent positive demonstrating greater resilience. conclusion, the optimization strategy not only accelerates the growth of economic indicators but also enhances system stability, providing a reliable path for regional economic development.

The DALYs lost in the optimized scenario drop significantly from 135.2 thousand person-years in 2015 to 86.7 thousand person-years in 2022, while the baseline scenario only slightly decreases from 135.2 to 137.9 during the same period. The gap between the two widens from zero to 51.2 thousand person-years. This change reveals that the optimization strategy's effect on reducing the disease burden has increased over time, attributed to the gradual implementation of health interventions. From the perspective of loss composition, the DALYs in the baseline scenario actually increase from 2016 to 2019, reflecting the cumulative effect of health risks in the non-optimized scenario, while the continued decline in the optimized scenario highlights its preventive advantage. The optimization strategy can effectively curb the expansion of health losses, and its long-term implementation can bring substantial improvements, providing data support for health-first policies.

### **CONCLUSION**

This study, through a comprehensive industrypollution-health analysis framework, empirically analyzes the spatial correlation between F pollution and industrial layout in the Yangtze River Economic Belt, demonstrating that regional collaborative governance can effectively address the spatial mismatch between high pollution and low health. However, present research does not fully consider the long-term impact of climate change on pollutant dispersion, and the dynamic evolution of industrial linkage networks needs to be further explored. Future research is needed to explore smart regulatory models enabled by digital technology and establish linkage mechanism between total F emission control and regional ecological compensation, innovative pathways for cross-basin collaborative governance.

### **FUNDING**

The financial support was provided by the Youth Project of National Social Science Fund of China (23TJC00363), Planning Project of China Commercial Economics Association (20252024), and Project for Improving the Scientific Research Foundation Ability of Young and Middle-aged Teachers in Guangxi Universities (2024KY0795).

# DISCLOSURE OF FINANCIAL AND NON-FINANCIAL RELATIONSHIPS AND ACTIVITIES AND CONFLICTS OF INTEREST

None

### **REFERENCES**

- [1] Thakur K, Ahmed M. Exploring the relationship between local governance and regional economic integration in the context of globalization. Lex Localis J Local Self-Govern. 2025;23(S1):239-244. DOI: 10.52152/
- [2] Mayasari D, Zubaidah I. Regional cooperation governance in urban economic development: A strategic study in Pangkalpinang city. J Public Representative Soc Provision 2025;5(3):587-599. DOI: 10.55885/jprsp.v5i3.632
- [3] Gianelle C, Guzzo F, Barbero J, Salotti S. The governance of regional innovation policy and its economic implications. The Ann Reg Sci. 2024;72(4):1231-1254. DOI: 10.1007/s00168-023-01241-2
- [4] He C, Sheng H. Governance capacity, related variety and regional economic resilience under the COVID-19 epidemic: evidence from China. The Ann Reg Sci. 2024;73(1):291-321. DOI: 10.1007/s00168-024-01266-1
- [5] Maharjan R. Decentralization and regional economic growth in Indonesia: An analysis of governance and fiscal decentralization. Law Econ. 2024;18(1):23-34.
- [6] Ogbuabor JE, Emeka ETG, Ogbuabor CA. Effects of entrepreneurship and governance quality on global and regional economic performance: A pathway to sustainable development. Sustainable Development, John Wiley & Sons, Ltd., 2025;33(2):2842-2863. DOI: 10.1002/sd.3267
- [7] Gunasekaran, Govindaraj R. Role of mega-regional trade agreements in fostering global economic governance. Ramanujan Int J Business Res. 2023;8(1):52-58. DOI: 10.51245/rijbr.v8i1.2023.1042
- [8] Ekeocha DO, Ogbuabor JE, Ogbonna OE, Orji A. Economic policy uncertainty, governance institutions and economic performance in Africa: are there regional differences?. Econ Change Restruct. 2023;56(3):1367-1431. DOI: 10.1007/s10644-022-09472-7
- [9] Fauji Z, Syafitri W. The impact of local governance and regional own-source revenue on economic growth at the district level in Indonesia. Jurnal Ekonomi dan Bisnis 2024;27(2):153-174. DOI: 10.24914/jeb.v27i2.11606
- [10] Suhendra A. SIPDD innovation (Regional Development Planning Information System) and ARABIKA CABINET (Arabica Coffee Integrated Economic Development Collaboration) as development governance innovation programs in South Sulawesi province and East Java province. Int J Regional Innov. 2021;1(4):32-40. DOI: 10.52000/ijori.v1i4.26
- [11] Hooijmaaijers B. China, the BRICS, and the limitations of reshaping global economic governance. The Pacific Rev. 2021;34(1):29-55. DOI: 10.1080/09512748.2019.1649298
- [12] Sutton J, Arcidiacono A, Torrisi G, Arku RN. Regional economic resilience: A scoping review. Progress Human Geography 2023;47(4):500-532. DOI: 10.1177\_03091325231174183
- [13] Elnaiem A, Mohamed-Ahmed O, Zumla A, Mecaskey J, Charron N, Abakar MF, et al. Global and regional governance of One Health and implications for global health security. The Lancet 2023;401(10377):688-704. DOI: 10.1016/S0140-6736(22)01597-5
- [14] Sachdeva L, Sharma R. Decentralized local governance and its impact on promoting economic development and reducing regional disparities. Lex localis-J Local Self-Govern. 2025;23(S1):164-168. DOI: 10.52152/
- [15] Fadilah SN. Implementation of governance with transparency and accountability in the gunung gambir rubber plantation of PTPN nusantara 1 regional 5 Islamic

- economic perspective. IJIEF: Indonesian J Islamic Econ Finance 2025;8(1):32-41. DOI: 10.35719/ijief.v8i1
- [16] Putra AP, Rio A. The influence of good corporate governance, regional original income, general allocation funds, capital expenditure and community welfare on economic growth in gresik district. WORLDVIEW (Jurnal Ekonomi Bisnis dan Sosial Sains) 2022;1(1):01-19. DOI: 10.38156/worldview.v1i1.116
- [17] Khan AT. Xi Jinping's economic diplomacy and china's influence on global governance: regional security implications. Int J Social Sci Res. 2024;1(1):11-19. DOI: 10.5281/zenodo.15804731
- [18] Liu K. Mechanism analysis of cross-regional collaborative governance of health resources in the twin-city economic circle of Chengdu-Chongqing region. Front Econ Manage. 2021;2(11):206-214. DOI: 10.6981/FEM.202111\_2(11).0028